Analytical methods for series compensation of a transmission line

Fabio Massimo Gatta [a], Davide Lauria [b], Stefano Quaia [c], Stefano Lauria [a,*]

[a] DIAEE, University of Rome Sapienza, Via Eudossiana 18, 00184 Rome, Italy
[b] Department of Industrial Engineering, University of Naples Federico II, via Claudio, 21, 80125 Napoli, Italy
[c] Department of Engineering and Architecture, University of Trieste, Via Valerio 10, 34127 Trieste, Italy

ARTICLE INFO

Keywords:
Series compensation
Line loadability
Active power flow control
Optimal power flow

ABSTRACT

The paper proposes an analytical approach to evaluate the effects of series compensation of an overhead transmission line (OHL) concerning the increase of (1) loadability and (2) practical loading of the line. The first part of the paper focuses only on the line characteristics, and proposes an analytical approach to determine the loadability curves of the line as a function of the compensating capacitive reactance. In the second part of the paper, the perspective shifts to examine the power loading of the selected OHL in a meshed electrical network. The target is to evaluate the compensation degree required to achieve a desired power flow increase in the line. To this purpose a fast analytical method, based on the compensation theorem, is presented. Preserving the linearity of the network model, the proposed method allows computation of the needed compensation degree by means of a closed form equation. Numerical applications performed on two simple test networks allow to compare the method with an ad hoc implemented classical optimal power flow. The results validate the method and highlight its effectiveness as a simple and useful tool to support power system planners and designers.

1. Introduction

The current evolution of power systems, mainly caused by the increasing penetration of renewable energy sources, concerns different items such as the reduction of short circuit power and system inertia, more stringent voltage regulation needs and others. This scenario pushes to revise the transmission networks planning criteria and/or change the existing networks according with specific local needs. Naturally, decisions about any network change require a full knowledge of the power system features, including a careful investigation of the power transfer capabilities of the lines. To this regard, the traditional load-flow and optimal power flow studies are the main available steady-state analysis tools.

Among the possibilities to expand/modify an existing transmission system, the connection of reactive power compensators and/or FACTS devices is generally preferred to the construction of new lines as it entails lower costs.

This work deals with capacitive series compensation of a transmission line, which is an effective means to increase the exploitation of the line. In the first part (Section 2), the paper deals with the line loadability increase obtainable through a series capacitance. The second part of this work (Sections 3-5) deals with evaluation of the series capacitance needed to obtain a desired power flow increase in the compensated line, included in a meshed power system. While the first part assumes (and is useful for) either a fixed or controllable series compensation, the second part implicitly assumes a controllable series compensation, since the desired power flow in the line changes over time according with load and generation scenarios.

The loadability of a transmission line is defined as the maximum power the line can carry in steady-state conditions. This maximum power is just a theoretical limit, since it is evaluated neglecting the practical constraints that always apply (e.g. like those imposed by the N-1 security criterion and by the transmission reliability margin). This concept was originally introduced in 1953 by St. Clair with respect to uncompensated OHLs. He derived the loadability curve, in per unit (p.u.) of the SIL, as a function of the line length, L [1]. Subsequent works extended the St. Clair loadability curve to the EHV and UHV lines [2]. Later, reference [3] reported the 'universal loadability curve' of uncompensated OHLs (in p.u. of the SIL), which can be applied, without loss of generality, to any voltage level. The technical constraints considered in the determination of the maximum power transmissible by the line are the thermal limit of conductors, the maximum permissible voltage drop, and the steady-state angle stability margin. Further studies have also taken into account Joule losses [4–6] and the dynamic line rating [7]. Beginning with [2], calculation of the loadability curves has

* Corresponding author.
E-mail address: stefano.lauria@uniroma1.it (S. Lauria).

Nomenclature

L	line length
L_1	maximum line length of the first loadability region for uncompensated lines
L_1'	maximum line length of the first loadability region for compensated lines
L_2	maximum line length of the second loadability region
$\dot{K}$	line propagation constant
$\dot{Z}_o$	line characteristic impedance
i_{th}	line thermal limit
Δv_{max}	maximum voltage drop across the line
P^*	desired active power flow in the compensated line
x_c	series capacitor reactance
x_l	line reactance
$K_s = x_c/x_l$	compensation degree

Abbreviations

OHL	overhead transmission line
FACTS	flexible AC transmission systems
SIL	surge impedance loading
EHV	extra high voltage
UHV	ultra-high voltage
VAR	volt-ampere reactive
TCSC	thyristor controlled series capacitors
ACSR	aluminium conductor steel reinforced
PST	phase shifter transformer
OPF	optimal power flow

been always performed through digital simulations.

The loadability curves identify different length ranges or 'regions'. In the first region, that concerns short lines, the transmissible power is limited by the conductor thermal limit. For uncompensated lines the maximum line length of the first region, L_1, extends up to about $L =$ 50–100 km depending on the conductors, line parameters, load power factor and voltage drop limit. For longer lines, the thermal limit is superseded the limit posed by the voltage drop across the line. The maximum voltage drop accepted defines a second region, usually wider than the first one, which can extend up to $L_2 = 500$ km, depending on the voltage drop limit, load power factor and stability margins. For even longer lines other constraints, such as steady-state angle, voltage stability margin, or the maximum accepted Joule losses, prevail.

All the above does not take into account reactive power management through VAR resources, which can increase loadability since it depends on the receiving-end power factor, which can be controlled by reactive power injections [8,9]. Controlled reactive compensation limits the voltage drop across the line and, thus, extends the first region, i.e. L_1 increases. The line loadability can be increased also by means of series capacitors, which compensate for the series reactance of the line [10].

In the first part (Section 2), this paper focuses the changes in the line loadability curves obtainable through a given capacitive series reactance. For calculation of the loadability curves, we propose an unusual analytical approach, completely different from the usual approach based on digital simulations. Analytical calculation of the loadability curves is not subject to limitations and can be a useful alternative mean to support power system planners.

In the second and more extended part of this work (Sections 3-5), the focus shifts from the (theoretical) loadability of a single line to the practical loading of the line as part of the electrical network. The target is to increase, through controllable series compensation, the power transported by a given line included in a meshed power system. Obviously, the problem becomes much wider as the whole power system and the relevant power flows are now concerned. To this regard, in Section 3 the authors present a novel methodology to solve the practical problem: "calculation of the compensation degree required to obtain a desired power flow in the compensated line". The novel methodology has the advantage to be simpler and faster than the optimal power flow classical approach. Note that all the analyses performed in this paper regard steady-state operation and, thus, the effects of series compensation do not concern the system transient stability.

Power flows in a meshed network can be controlled adjusting the parameters that govern the line behavior, such as series impedance [11,12], or magnitude and angle of the bus voltages. This can be done using FACTS devices, a family of electronic devices that includes also the TCSC, which provides controllable series compensation. Series compensation has been successfully utilized for many years in electric power networks, mainly to enhance angular transient stability, voltage stability, as well as power flows among parallel EHV-OHLs with different reactances. With series compensation, it is possible to increase the transfer capability of existing power transmission systems at a lower investment cost and with a shorter installation time compared to the building of new, additional lines. With the advent of thyristor control, the concept of series compensation has been widened and its usefulness has been increased further. TCSC configurations comprise controlled reactors in parallel with sections of a capacitor bank. This combination allows smooth control of the fundamental frequency capacitive reactance over a wide range. TCSC introduce a number of further important benefits in the application of series compensation: elimination of subsynchronous resonance risks, damping of active power oscillations, post-contingency stability improvement, dynamic power flow control. The overall result typically appears as increased transfer capacity. Several papers deal with the general topic of network optimal utilization by using TCSCs [13–27]. TCSCs have been proposed to meet a variety of objectives that include the increase of power transfer capability [13,14], enhancement of power system loadability [15–20], power loss reduction [22,23], voltage stability improvement [22], fuel cost and emission reduction [23], congestion management [24,25], reactive power planning [26].

In Section 3.1, this work proposes a novel analytical method, based on the compensation theorem, for evaluation of the series compensation degree required to obtain a desired power flow increase in the compensated line. Under mild assumptions, the proposed method allows to solve this complex problem by means of a linear formulation. It follows that, compared to traditional optimal power flow procedures (sketched for comparison in Section 3.2), the analytical method proposed is simpler and faster. In Sections 4-5, the novel analytical method is validated by comparison with the traditional constrained optimization method outlined in Section 3.2. For this purpose, numerical applications are performed on two simple meshed networks. Section 4 includes the description of the two test networks (whose parameters are listed in the Appendix) and reports the relevant test scenarios and the results obtained with the proposed analytical method. Section 5 compares the results obtained through the novel method proposed and the traditional optimization method. The accuracy and robustness of the novel analytical method are demonstrated also by the results of some sensitivity analyses reported in the same Section 5.

To sum up, the novelty and main contribution of this paper include:

- the alternative analytical approach presented for line loadability calculation of series compensated lines;

- the analytical method, based on the compensation theorem, for calculation of the series capacitance required to obtain a desired power flow increase in the compensated line. The proposed method is simpler and faster than a traditional optimal power flow study. The method can

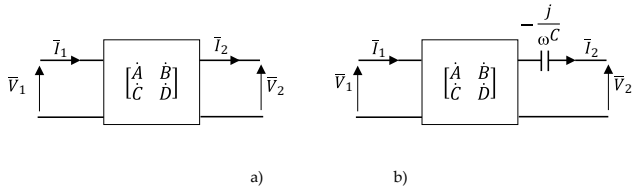

Fig. 1. Equivalent circuits of (a) uncompensated and (b) series compensated lines.

be particularly efficient and convenient at the planning stage. For example, the simplicity of formulation allows to carry out fast sensitivity analyses that can support power system planners and designers.

2. Loadability of transmission lines

2.1. Loadability of uncompensated lines

The effectiveness of capacitive series compensation to increase the transmission capability of OHLs is clearly shown by the loadability curves. These curves usually are numerically computed but can be also analytically derived as shown in [28] and briefly recalled here. For the typical line lengths of the Italian transmission network (less than 300 km), the only constraints of interest are the conductor thermal limit and the voltage drop limit. Accordingly, in what follows we consider only the first two regions of the loadability curves. The analytical formulation of power transmission lines can be expressed in the standard compact form (Fig. 1a):

$$\begin{cases} \bar{V}_1 = \dot{A}\bar{V}_2 + \dot{B}\bar{I}_2 \\ \bar{I}_1 = \dot{C}\bar{V}_2 + \dot{A}\bar{I}_2 \end{cases} \tag{1}$$

with:

$\dot{A} = \cosh(\dot{K}L)$, $\dot{B} = \dot{Z}_o \sinh(\dot{K}L)$, $\dot{C} = \left(1/\dot{Z}_o\right)\sinh(\dot{K}L)$, where $\dot{K}$ is the propagation constant and $\dot{Z}_o$ is the characteristic impedance of the line. In the following, the quantities will be expressed in p.u. and, consequently, they will be denoted by lowercase letters.

In the first loadability region, determined by the thermal limit, the magnitude of the sending end current is slightly lower than that of receiving end, as well as at any point of the line. The thermal constraint is, therefore, attained at the line receiving end.

If i_{th} is the conductor thermal limit, by denoting the attendant apparent power with $a_{th} = v_2 i_{th}$, the maximum allowable active power is $p_{th} = a_{th}\cos\varphi_2$, where $\cos\varphi_2$ is the load power factor.

By assuming $\bar{v}_2 = v_2 e^{j0} = v_2$, the following expression:

$$\bar{v}_1 = v_2 \cosh(\dot{K}L) + \frac{p_{th}}{v_2}(1 - j\tan\varphi_2)\dot{z}_o \sinh(\dot{K}L) \tag{2}$$

wholly characterizes the first region.

The thermal limit prevails until the voltage drop limit Δv_{max} is reached at the line length L_1, which can be determined by solving the nonlinear equation:

$$v_1^{\max} = \left| v_2 \cosh(\dot{K}L_1) + \frac{p_{th}}{v_2}(1 - j\tan\varphi_2)\dot{z}_o \sinh(\dot{K}L_1) \right| \tag{3}$$

imposing $v_1^{max} = v_2 + \Delta v_{max}$.

The second region of the loadability curve, for $L > L_1$, is dictated by the voltage drop limit. The maximum transmissible active power $p(L)$ is a function of L and can be determined by solving the algebraic quadratic equation:

$$v_1^{\max} = \left| v_2 \cosh(\dot{K}L) + \frac{p}{v_2}(1 - j\tan\varphi_2)\dot{z}_o \sinh(\dot{K}L) \right| \tag{4}$$

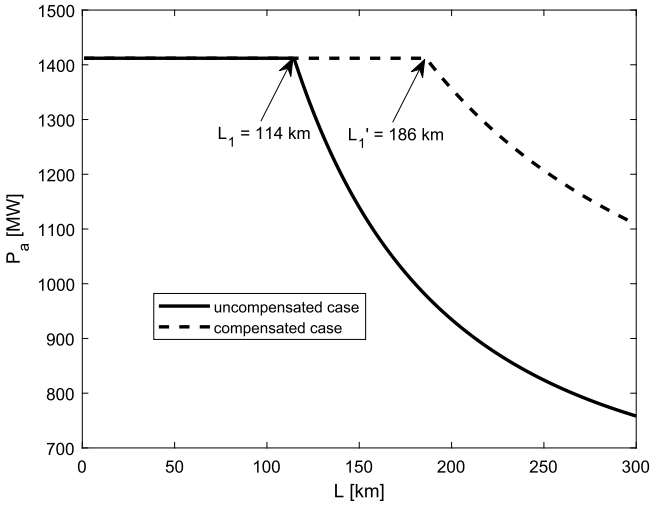

Fig. 2. Loadability curves of uncompensated and series compensated OHLs (x_c = 20 Ω).

2.2. Loadability of series compensated lines

When a series capacitor bank having reactance x_c is located at the receiving end of the OHL, as illustrated in Fig. 1.b, the transmission equations of the line become:

$$\begin{cases} \bar{V}_1 = \dot{A}\bar{V}_2 + \left(\dot{B} - jx_c\dot{A}\right)\bar{I}_2 \\ \bar{I}_1 = \dot{C}\bar{V}_2 + \left(\dot{A} - jx_c\dot{C}\right)\bar{I}_2 \end{cases} \tag{5}$$

As the series compensation reduces the overall voltage drop along the line, it extends the first region of the loadability curve up to a length $L_1' > L_1$, which depends on the adopted compensation degree $K_s = x_c/x_l$.

For a given value x_c of the capacitor bank reactance, the length L_1' for which the voltage drop limit is attained can be determined by solving the equation in the unknown L:

$$v_1^{\max} = \left| v_2 \cosh(\dot{K}L) + \frac{p}{v_2}(1 - j\tan\varphi_2)\left(\dot{z}_o \sinh(\dot{K}L) - jx_c \cosh(\dot{K}L)\right) \right| \tag{6}$$

Conversely, the reactance x_c required to extend the first region boundary to a given line length $L > L_1$ can be found by solving the algebraic equation (6) in the unknown x_c.

Fig. 2 shows the loadability curves, computed for $L \leq 300$ km, for an

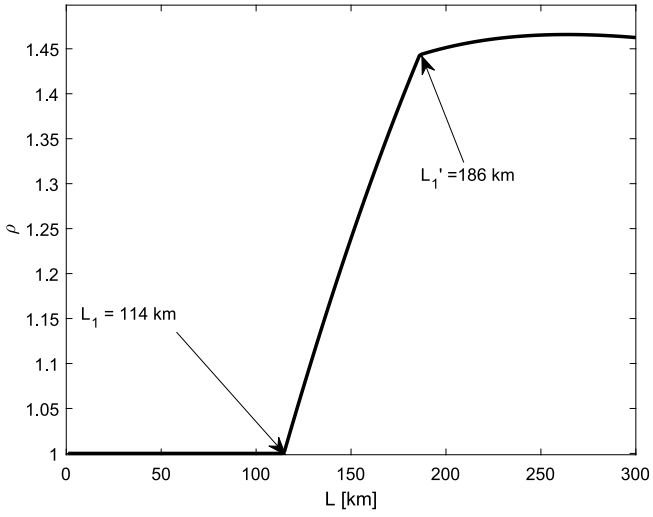

Fig. 3. Ratio of series compensated/uncompensated loadability curves (x_c = 20 Ω).

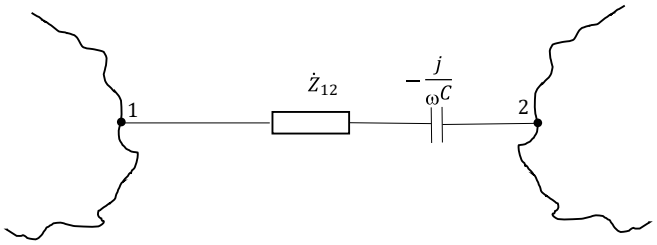

Fig. 4. Series compensation scheme applied to the line 1–2 of a meshed network.

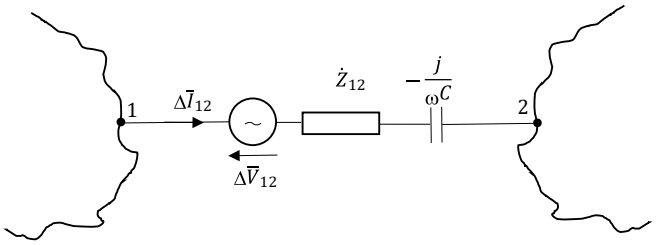

Fig. 5. Current change $\Delta\bar{I}_{12}$ due to the insertion of the impedance $-j/\omega c$.

Fig. 6. Current injections $-\Delta\bar{I}_{12}$ and $\Delta\bar{I}_{12}$ into the two ends of the target line.

OHL equipped with triple ACSR conductor bundles (3x585 mm^2 cross section). The electrical line constants are $r = 0.021$ Ω/km, $x_l = 0.271$ Ω /km, $g = 0.004{\cdot}10^{-6}$ S/km, $b = 4.21{\cdot}10^{-6}$ S/km.

Computations are based on the following assumptions:

- thermal limit $i_{th} = 2038$ A, i.e. the most conservative value reported in the Italian Standard 11–60 [29]);
- voltage drop limit $\Delta v_{max} = 5$ %;
- receiving end constant voltage $V_2 = 400$ kV;
- load power factor (at the receiving end) $\cos\varphi_2 = 1$;
- capacitor reactance $x_c = 20$ Ω ($Q_n = 250$ MVAR).

For any other power factor value, the loadability curves can be easily recalculated.

Fig. 2 shows that the loadability increase of the compensated line is significant in a range of lengths of high practical interest: the first region limit lengths are respectively $L_1 = 114$ km for the uncompensated line and L_1'=186 km (with a 63 % increase) for the compensated line. For example, with $x_c = 20$ Ω ($K_s = 0.369$) a 200 km long OHL could transport about 45 % more power, as one can see both in Fig. 2 and in Fig. 3, which highlights the power loadability increase due to the series compensation.

Finally, we point out that the analytical method presented can support power system planners, being a fast and accurate alternative mean for calculation of the loadability curves.

3. Power flow increase by series compensation in a selected line of a meshed network

The most direct way to face heavy load increases consists in the exploitation of the existing reactive resources of the system. However, when the existing reactive resources are not sufficient, transmission network reinforcements become imperative. As highlighted in the introduction, FACTS or PST devices are recognized as powerful means to get high benefits. The choice of the most convenient device is outside the scope of this paper, but the analysis of the relevant literature clearly shows that series compensation is a suitable solution to improve power transmission in meshed networks. In the steady-state perspective of this work (and, thus, without considering transient stability considerations), series capacitors can be used, as well known, to improve active power flows. For example, overloads in critical lines can be avoided and the overall system safety increased.

In practice, it is important that proper models, methods and tools, able to address engineering challenges avoiding burdensome evaluations, are made available to planners. To this regard, the choice and sizing of a FACTS device can be made in the most correct way resorting to constrained optimization procedures. However, optimization procedures often require a significant effort, and thus the availability of simpler tools can be important to get faster well approximated results. In this framework, the novel contribution of this paper consists in the proposal of a simple analytical method, alternative to the traditional optimization methods, that can support planners at a first analysis stage. In order to calculate the capacitive series compensation degree required to exploit a selected line at a convenient load level, a simple, fast and linear formulation of the system model, based on the compensation theorem, is proposed in Section 3.1. The solution of the same problem with a traditional optimal power flow procedure is outlined in Section 3.2.

3.1. *Computation of the series compensation degree using the compensation theorem*

Let us suppose that the series capacitor is located between bus 1 and 2 of a meshed transmission grid, as shown in Fig. 4.

Let $\bar{I}_{12}$ be the current flowing in the branch 1–2 without the compensation. According to the compensation theorem, the current change $\Delta\bar{I}_{12}$ in the 1–2 branch due to the addition of the series capacitive impedance = $-j/(\omega C)$ can be evaluated by inserting in the 1–2 branch the voltage source $\Delta\bar{V}_{12} = -j\bar{I}_{12}/(\omega C)$ in series with the impedance $-j/(\omega C)$, and replacing all other sources with their equivalent impedances as shown in Fig. 5.

In what follows, all the PQ buses and PV buses are modeled as current sources and the slack bus as an ideal voltage source, i.e. $\Delta V_n = 0$.

Suppose, without loss of generality, that the balance node is the last one. As a consequence, the electrical network is described by the nodal admittance matrix, evaluated by removing branch 1–2 as shown in Fig. 6.

For the branch 1–2 the following relationship can be then written:

$$\Delta\bar{I}_{12} = \frac{\Delta\bar{V}_1 - \Delta\bar{V}_2 - \Delta\bar{V}_{12}}{\dot{Z}_{12} - \frac{j}{\omega C}} \tag{7}$$

where $\Delta\bar{V}_1$ and $\Delta\bar{V}_2$ are the voltage variations at buses 1 and 2 of the passivated network due to the inserted impedance $-j/\omega C$, and $\Delta\bar{V}_{12}$ is the compensation voltage source. The network model can thus be formulated using the nodal Maxwell law:

$$\begin{aligned}
&\dot{Y}_{11}\Delta\bar{V}_1 + \dot{Y}_{12}\Delta\bar{V}_2 + \cdots\ldots\dot{Y}_{1,n-1}\Delta\bar{V}_{n-1} = -\Delta\bar{I}_{12}\\
&\dot{Y}_{21}\Delta\bar{V}_1 + \dot{Y}_{22}\Delta\bar{V}_2 + \cdots\ldots\dot{Y}_{2,n-1}\Delta\bar{V}_{n-1} = \Delta\bar{I}_{12}\\
&\qquad\cdots\qquad\qquad\cdots\qquad\qquad\cdots\\
&\dot{Y}_{n-1,1}\Delta\bar{V}_1 + \dot{Y}_{n-1,2}\Delta\bar{V}_2 + \cdots\ldots\dot{Y}_{n-1,n-1}\Delta\bar{V}_{n-1} = 0\\
&\dot{Y}_{n,1}\Delta\bar{V}_1 + \dot{Y}_{n,2}\Delta\bar{V}_2 + \cdots\ldots\dot{Y}_{n,n-1}\Delta\bar{V}_{n-1} = \Delta\bar{J}_n
\end{aligned} \tag{8}$$

In a compact form, the previous model can be rewritten as:

$$\begin{aligned}\dot{Y}_1\Delta\bar{V}_s+\dot{Y}_2\Delta\bar{V}_r&=\Delta\bar{J}\\ \dot{Y}_3\Delta\bar{V}_s+\dot{Y}_4\Delta\bar{V}_r&=0\\ \dot{Y}_5\Delta\bar{V}_s+\dot{Y}_6\Delta\bar{V}_r&=\Delta\bar{J}_n\end{aligned}\tag{9}$$

where

$$\Delta V_s^T=[\Delta\bar{V}_1\quad\Delta\bar{V}_2],\ \Delta V_r^T=[\Delta\bar{V}_3\quad\Delta\bar{V}_4\quad\dots\quad\Delta\bar{V}_{n-1}],\ \Delta\bar{J}^T=[-\Delta\bar{I}_{12}\quad\Delta\bar{I}_{12}],$$

$$\left[\dot{Y}_1\right]=\begin{bmatrix}\dot{Y}_{11}&\dot{Y}_{12}\\ \dot{Y}_{21}&\dot{Y}_{22}\end{bmatrix},\ \left[\dot{Y}_2\right]=\begin{bmatrix}\dot{Y}_{13}&\cdots&\dot{Y}_{1,n-1}\\ \dot{Y}_{23}&\cdots&\dot{Y}_{2,n-1}\end{bmatrix}=\left[\dot{Y}_3\right]^T,$$

$$\left[\dot{Y}_4\right]=\begin{bmatrix}\dot{Y}_{33}&\cdots&\dot{Y}_{3,n-1}\\ \cdots&\cdots&\cdots\\ \dot{Y}_{n-1,3}&\cdots&\dot{Y}_{n-1,n-1}\end{bmatrix},\left[\dot{Y}_5\right]=\left[\dot{Y}_{n,1}\quad\dot{Y}_{n,2}\right],\ \left[\dot{Y}_6\right]=\left[\dot{Y}_{n,3}\quad\cdots\quad\dot{Y}_{n,n-1}\right]$$

Since the second of (9) yields$\Delta\bar{V}_r=-\dot{Y}_4^{-1}\dot{Y}_3\Delta\bar{V}_s$, by substituting it in the first relationship of (9) the following reduced system is obtained:

$$\left(\dot{Y}_1-\dot{Y}_2\dot{Y}_4^{-1}\dot{Y}_3\right)\Delta\bar{V}_s=\dot{Y}_{red}\Delta\bar{V}_s=\Delta\bar{J}\tag{10}$$

being: $\dot{Y}_{red}=\left(\dot{Y}_1-\dot{Y}_2\dot{Y}_4^{-1}\dot{Y}_3\right)$

By defining: $\dot{Z}_{red}=\dot{Y}_{red}^{-1}$, it follows

$$\Delta\bar{V}_S=\dot{Z}_{red}\Delta\bar{J}\Rightarrow\begin{bmatrix}\Delta\bar{V}_1\\ \Delta\bar{V}_2\end{bmatrix}=\begin{bmatrix}\dot{Z}_{red,11}&\dot{Z}_{red,12}\\ \dot{Z}_{red,21}&\dot{Z}_{red,22}\end{bmatrix}\begin{bmatrix}-\Delta\bar{I}_{12}\\ \Delta\bar{I}_{12}\end{bmatrix}\tag{11}$$

Taking into account (7), the current $\Delta\bar{I}_{12}$ is expressed in turn as:

$$\Delta\bar{I}_{12}=\frac{\frac{j\bar{I}_{12}}{\omega C}}{\dot{Z}_{red,11}+\dot{Z}_{red,22}-\dot{Z}_{red,12}-\dot{Z}_{red,21}+\dot{Z}_{12}-\frac{j}{\omega C}}\tag{12}$$

from which expressions of $\Delta\bar{V}_1$ and $\Delta\bar{V}_2$ can be carried out as a function of the unknown capacitance C, whereas the other quantities are all known:

$$\begin{aligned}\Delta\bar{V}_1&=-\frac{\frac{j\bar{I}_{12}}{\omega C}\left(\dot{Z}_{red,11}-\dot{Z}_{red,12}\right)}{\dot{Z}_{red,11}+\dot{Z}_{red,22}-\dot{Z}_{red,12}-\dot{Z}_{red,21}+\dot{Z}_{12}-\frac{j}{\omega C}}\\ \Delta\bar{V}_2&=\frac{\frac{j\bar{I}_{12}}{\omega C}\left(\dot{Z}_{red,22}-\dot{Z}_{red,21}\right)}{\dot{Z}_{red,11}+\dot{Z}_{red,22}-\dot{Z}_{red,12}-\dot{Z}_{red,21}+\dot{Z}_{12}-\frac{j}{\omega C}}\end{aligned}\tag{13}$$

Finally, the value of the capacitance C required to ensure the desired active power flow P^* along the branch 1–2 can be evaluated by solving the equation:

$$Re\{(\bar{V}_1+\Delta\bar{V}_1)(\bar{I}_{12}+\Delta\bar{I}_{12})^*\}-P^*=0\tag{14}$$

Expressing P^* in terms of the power increase ΔP^*, i.e. $P^*=P_{12}+\Delta P^*$, where $P_{12}=Re\{\bar{V}_1\bar{I}_{12}^*\}$ is the active power without compensation, and setting:

$$x_c=\frac{1}{\omega c}$$

$$\Delta\bar{I}_{12}=\frac{\dot{\alpha}x_c}{\dot{\beta}-jx_c},\ \text{with}\ \dot{\alpha}=j\bar{I}_{12},\ \dot{\beta}=\dot{Z}_{red,11}+\dot{Z}_{red,22}-\dot{Z}_{red,12}-\dot{Z}_{red,21}+\dot{Z}_{12};$$

$$\Delta\dot{V}_1=\dot{\gamma}\Delta\bar{I}_{12},\ \text{with}\ \dot{\gamma}=-\left(\dot{Z}_{red,11}-\dot{Z}_{red,12}\right);$$

$$\dot{V}_1=\dot{k}$$

after simple manipulations the following quadratic equation in the unknown x_c can be obtained:

$$\begin{aligned}&\left(Re\left\{-j\dot{k}\dot{a}^*+j\dot{\gamma}\dot{a}\bar{I}_{12}^*+\dot{\gamma}I_{12}^2\right\}-\Delta P^*\right)x_c^2+\left(Re\left\{\dot{k}\dot{a}^*\dot{\beta}\right.\right.\\ &\left.\left.+\dot{\gamma}\dot{a}\bar{I}_{12}^*\dot{\beta}^*\right\}\right)x_c-\beta^2\Delta P^*=0\end{aligned}\tag{15}$$

This demonstrates the simplicity of the proposed approach, since the calculation of the compensation degree needed to obtain the desired active power increase ΔP^* is reduced to the resolution of (15) in the only unknown x_c.

The proposed procedure can be synthetically visualized through the flowchart reported in Fig. 7.

3.2. *Computation of the series compensation degree using the optimal power flow (OPF)*

The procedure described in Section 3.1 allows a fast and simple computation of the series compensation degree required to ensure an assigned active power flow in a selected transmission line. This section outlines the solution of the same problem with a canonical methodology widely recognized in the relevant literature. The optimal power flow formulation, due to its versatility and generality, is chosen for this role.

At this purpose, let us consider a transmission network with $n+N=N_t$ buses, with n generation buses and N load buses, where series compensation is introduced on a certain branch. Lowercase letters mean that relevant quantities are expressed in p.u. By denoting with $\bar{v}_h$ the voltage at the node h, $\bar{i}_h$ the corresponding nodal current and $\dot{y}$ the network nodal admittance matrix, the fundamental matrix relationship maintains:

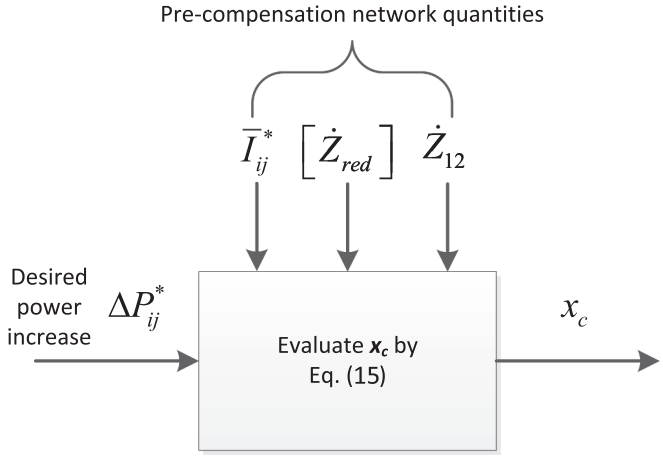

Fig. 7. Input data and output of the proposed procedure.

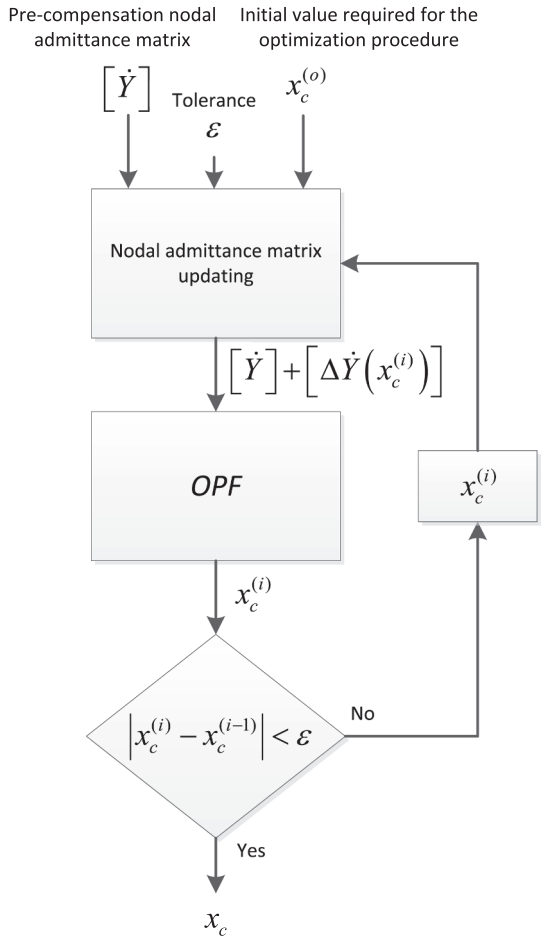

Fig. 8. Flow chart of the OPF procedure.

$$\bar{i} = \dot{y}\,\bar{v} \tag{16}$$

The admittance matrix is function of the actual reactance of the capacitor bank, which can be regarded as the only one control variable u. With reference to the n generation buses, the injected powers are related to the previously mentioned quantities by these relationships ($h = 1 \ldots n$).

$$\begin{cases} p_h = Re\left(\bar{v}_h \bar{i}_h^*\right) \\ q_h = Im\left(\bar{v}_h \bar{i}_h^*\right) \end{cases} \tag{17}$$

The nodal active powers at the generation buses are given as input data, except in the slack node. All the generator voltages are assumed equal to the ones in the base case without series compensation. The active and the reactive powers at the N load buses are assigned:

$$\begin{cases} p_h = Re\left(\bar{v}_h \bar{i}_h^*\right) = p_h^c \\ q_h = Im\left(\bar{v}_h \bar{i}_h^*\right) = q_h^c \end{cases} \tag{18}$$

The load flow variables are globally denoted by the vector x. The determination of the unknown compensating reactance can be integrated with the optimization procedure, choosing the objective function in the following way: by denoting with (i, k) the nodes corresponding to the branch for which a loading p^* is requested, the following objective function to be minimized can be stated:

$$\Phi = (p_{ik} - p^*)^2 \tag{19}$$

Hence, the optimization problem can be expressed in the classical and compact form of a constrained minimization problem:

$$\begin{aligned} &\min \Phi(\boldsymbol{x}, \boldsymbol{u}) \\ &\boldsymbol{f}(\boldsymbol{x}, \boldsymbol{u}) = 0 \\ &\boldsymbol{g}(\boldsymbol{x}, \boldsymbol{u}) \leqslant 0 \end{aligned} \tag{20}$$

where the vector functions $\boldsymbol{f}(\boldsymbol{x},\boldsymbol{u})$ and $\boldsymbol{g}(\boldsymbol{x},\boldsymbol{u})$ are relative to the equality and inequality constraints.

The OPF procedure is summarized in the Fig. 8 flowchart. The tolerance ε should be chosen case-by-case. For example, a reasonable range for ε could be [0.5,1] % of x_c, having in mind that the lower ε, the higher the number of iterations.

4. Numerical applications

In order to demonstrate the usefulness of the methodology described in the above section 3.1 and the accuracy of the relevant results, two different networks have been considered i.e.:

(i) the 6-node 400 kV test network with 7 OHLs depicted in Fig. 9a.
(ii) the 9-node 230 kV IEEE (WSCC) network slightly modified as reported in Fig. 9b.

The parameters of both networks are reported in the Appendix. For

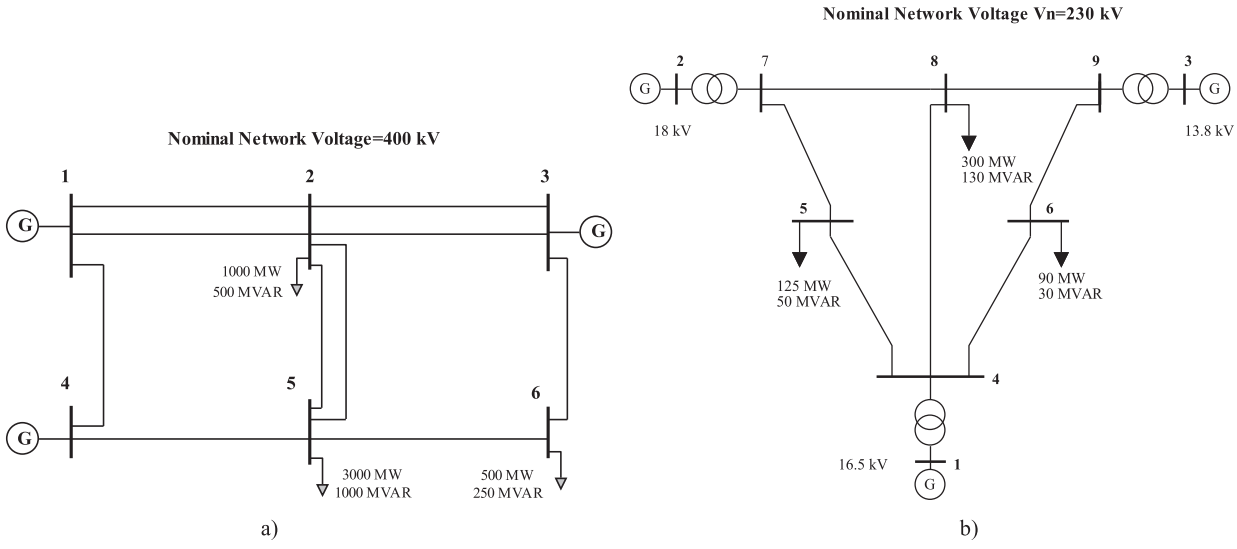

Fig. 9. (a) 400 kV 6-nodes test network; (b) 230 kV 9-nodes modified IEEE test network.

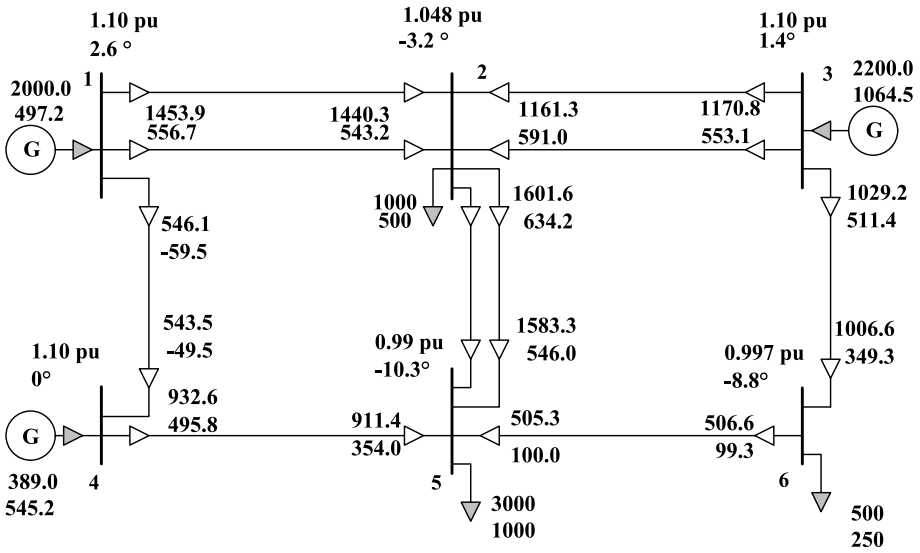

Fig. 10. 400 kV 6-node test network. Base case load flow. Voltages are in p.u. of 400 kV; powers in MW and MVAR.

Table 1
400 kV test nework. Base case load flow results.

Line	Line current (*A*)	Line current/thermal limit ratio
1–2	2120/2	0.52
3–2	1795/2	0.44
1–4	721	0.53
2–5	2442/2	0.60
3–6	1543	***1.14***
4–5	1425	***1.05***
6–5	751	0.57

Table 2
400 kV test network. Line 2–5 series capacitor reactance and compensation degree, for different target flow values.

Desired active power flow increase in line 2–5, k	Capacitor reactance x_c [Ω] and compensation degree K_s [p.u.] yielded by the compensation theorem, x_c/K_s
1.10	3.81/0.29
1.15	5.46/0.41
1.20	6.97/0.52
1.25	8.36/0.63
1.30	9.64/0.73
1.35	10.84/0.81

computation, both the proposed method and the optimal power flow have been implemented in Matlab.

4.1. 6-node 400 kV test network

Assuming the following load level: 1000 MW, 500 MVAR at node 2, 3000 MW, 1000 MVAR at node 5 and 500 MW, 250 MVAR at node 6, the base network load flow, without series compensation, is reported in Fig. 10, with the generator voltage settings chosen in order to minimize power system losses.

Table 1 reports the base case loading levels of the 7 OHLs. Clearly, system operation is not satisfactory because lines 3–6 and 4–5 are overloaded (respectively 114 % and 105 % of the 2038 A thermal limit already considered in Section 2.2), whereas the other lines are relatively lightly loaded.

Power flows in the lines 3–6 and 4–5 can be reduced by forcing more power through the OHL 2–5, which is selected for series compensation. In order to increase the active power flow in the line 2–5, the method based on the compensation theorem described in section 3.1 has been applied. Resolution of (15) provides the results listed in Table 2 as a function of the increase factor k of the active power carried by the line 2–5. Column 2 reports the required values of capacitive reactance x_c and the corresponding compensation degree K_s (the overall reactance of the double circuit line 2–5 in the base case is 13.3 Ω).

Note that k values higher than 1.25 require high compensation degrees, which can be considered not realistic in practice. Fig. 11 reports the load flow results in the case $k = 1.2$ (requiring an acceptable compensation degree $K_s = 0.52$), and Table 3 reports the relevant OHLs loading.

Comparing the columns III of Tables 1 and 3 it can be noted that after compensation the currents in lines 3–6 and 4–5 are reported below their thermal limits (94 % and 87 % respectively), while the current flowing in the line 2–5 is increased by about 17 %, up to 70 % of its thermal limit. Of course, the same procedure can be easily repeated selecting a different line for series compensation.

4.2. 9-node 230 kV modified IEEE test network

The second test network used is a modified version of the WSCC (or IEEE) standard 9-bus system, as shown in Fig. 9b. Despite the higher number of buses compared with the above reported 400 kV test network, the original 9-bus system is composed by only one mesh, and this makes it a rather poor transmission network in the perspective of a load flow analysis. Therefore, a new line has been added between bus 4 and bus 8, thus creating a second mesh and making the network more flexible for power flows analysis. Moreover, in order to increase somehow the power flows, the base case load at bus 8 has been increased compared to the original network, as highlighted in the Appendix.

Base case results, reported in Fig. 12, show an acceptable overall behavior with no violations. In order to increase the power transfer across line 4–8, series compensation has been added to the same line. Table 4 summarizes compensation values yielded by the proposed analytical method in order to attain different target flow values on line 4–8. As shown in Table 4, k values in the [1.10, 1.35] range dictate compensation degrees K_s spanning a [0.18, 0.51] interval, which are realistic and commonly encountered in practice.

Proceeding similarly to what has been done with the 6-bus network, assume the target to increase by 30 % the active power transported by line 4–8 ($k = 1.3$). In this case, the proposed analytical method provides $x_c = 40.94$ Ω that corresponds to $K_s = 0.46$ (Table 4).

The load flow results with $x_c = 40.94$ Ω are reported in Fig. 13. The

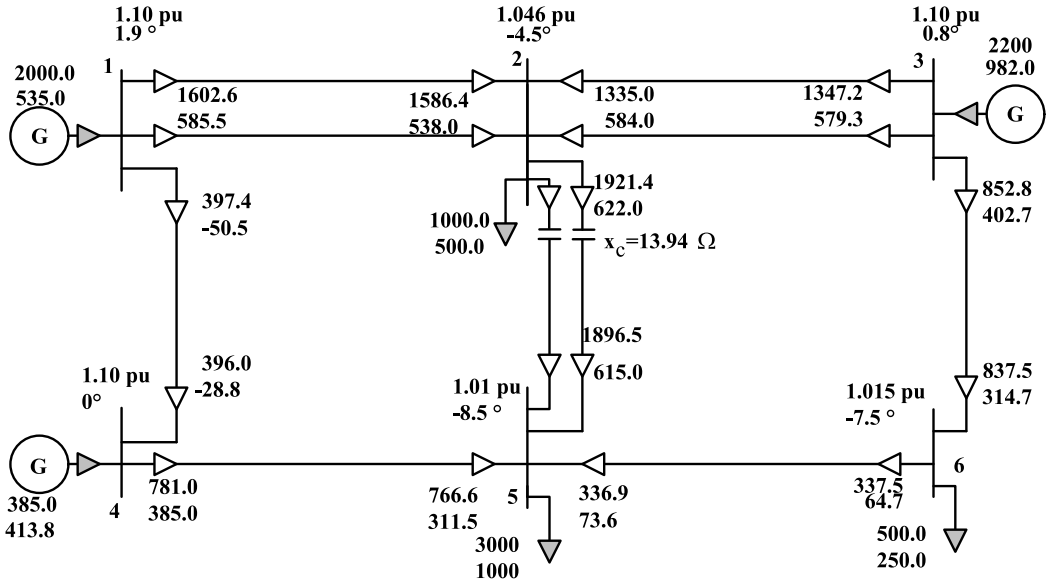

Fig. 11. 400 kV test network. Load flow with compensated line (case: k = 1.2). Voltages are in p.u. of 400 kV, powers in MW and MVAR.

Table 3
400 kV test network. Load flow results with $k = 1.2$ ($K_s = 0.52$).

Line	Line current (A)	Line current/thermal limit ratio
1–2	2311/2	0.57
3–2	2011/2	0.49
1–4	525	0.39
2–5	2849/2	0.70
3–6	1272	0.94
4–5	1183	0.87
6–5	493	0.36

active power flow on the line 4–8 is 109.7 MW at the sending end (bus 4) and 106.9 MW at the receiving end (bus 8). Without compensation, Fig. 12 shows that the line 4–8 transports about 82 MW: 83.1 MW at the sending end (bus 4) and 81.5 MW at the receiving end (bus 8). Therefore, the obtained increase of active power transported is about 31–32 %, very close to the 30 % target value.

5. Comparison between the proposed analytical method and OPF results

In order to evaluate the accuracy of the proposed analytical method, this section compares the values of the capacitive reactance x_c obtained

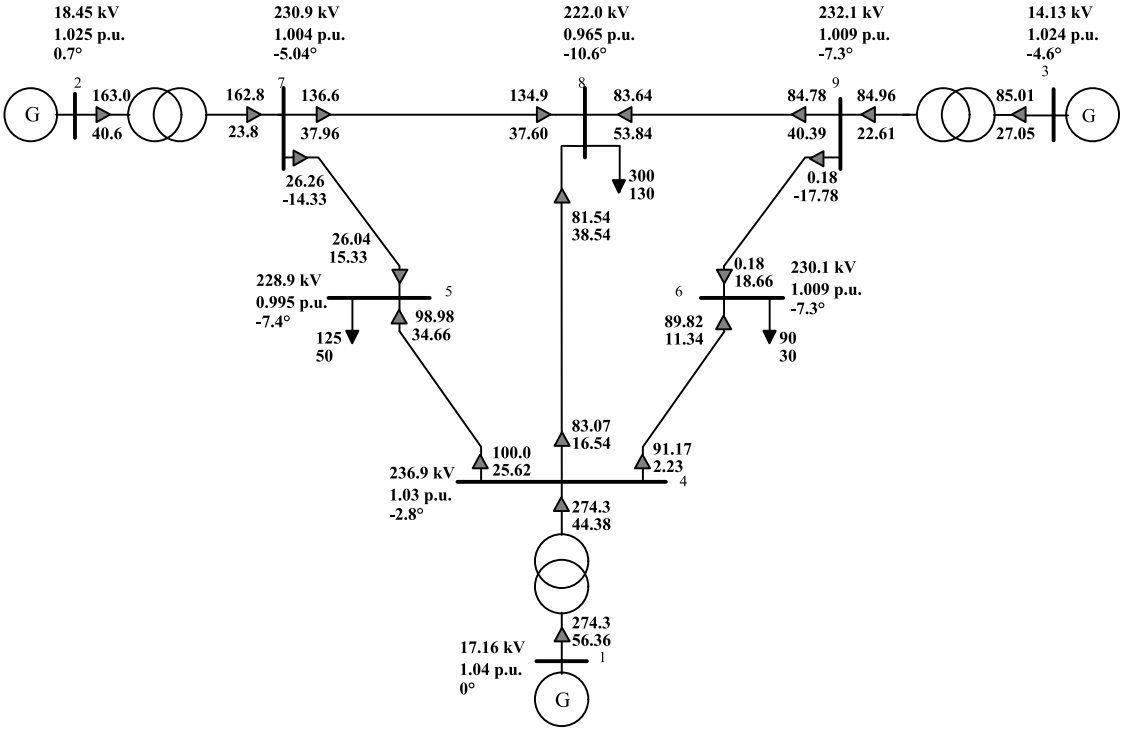

Fig. 12. 9-bus, 230 kV modified IEEE network. Base case load flow results, no series compensation.

Table 4
230 kV test network. Line 4–8 series capacitor reactance and compensation degree for different target flow values.

Desired active power flow increase in line 4–8, k	Capacitor reactance x_c [Ω] and compensation degree K_s [p.u.] yielded by the compensation theorem, x_c/K_s
1.10	16.03/0.18
1.15	23.06/0.26
1.20	29.46/0.33
1.25	35.44/0.39
1.30	40.94/0.46
1.35	46.02/0.51

by the solution of (15) and the OPF procedure described in Section 3.2, for different target values of active power increase in the compensated line, k. Table 5 reports the comparison of results between the proposed procedure and the OPF for the 6-bus 400 kV network, evidencing mismatches below 2 %.

The comparison for the 9-bus 230 kV network is reported in Table 6: in this case mismatches do not exceed 3.2 %.

The values of the capacitive reactance x_c computed with the proposed method and with the OPF are also plotted as a function of the power increase factor k in Fig. 14 for the 400 kV test network and in Fig. 15 for the 230 kV test network.

In order to check the effectiveness of the proposed method, several different simulations have been carried out, changing various system parameters in the two test networks. For reasons of space, only the results of some of the sensitivity analyses performed on the 9-bus IEEE test network are reported here. They refer to the following two cases:

(1) Outage of one out of two generators supposed in service at node 2: we assume that the active power generated at node 2 halves (from 163 MW to 82 MW). Without compensation, in this new generation scenario the active power transported by the line 4–8 is $P = 118.2$ MW. In order to increase this power up to the line SIL equal to 148 MW (thus, P^*=148 MW, $k = 1.25$), the capacitive reactance yielded by the proposed analytical method is $x_c = 36.24\ \Omega$, whereas the OPF gives $x_c = 34.88\ \Omega$. The error is 3.9 %.

(2) Load change at node 8: we assume P = 200 MW and Q = 85 MVAR (base case values are $P = 300$ MW and $Q = 130$ MVAR). Without compensation, in this new load scenario the active power transported by the line 4–8 is $P = 35.3$ MW. In order to

Table 5
400 kV test network. Comparison between x_c/K_s values yielded by the proposed procedure and by the OPF.

Capacitor reactance x_c [Ω] and compensation degree K_s [p.u.] yielded by the compensation theorem, x_c/K_s	Capacitor reactance x_c [Ω] and compensation degree K_s [p.u.] yielded by the OPF, x_c/K_s	Reactance x_c difference with respect to the OPF method [%]
3.81/0.29	3.74/0.28	1.9
5.46/0.41	5.37/0.40	1.6
6.97/0.52	6.86/0.51	1.5
8.36/0.63	8.24/0.62	1.1
9.64/0.73	9.52/0.72	1.3
10.84 /0.81	10.70 /0.80	1.3

Table 6
230 kV test network. Comparison between x_c/K_s values yielded by the proposed procedure and by the OPF.

Capacitor reactance x_c [Ω] and compensation degree K_s [p.u.] yielded by the compensation theorem, x_c/K_s	Capacitor reactance x_c [Ω] and compensation degree K_s [p.u.] yielded by the OPF, x_c/K_s	Reactance x_c difference with respect to the OPF method [%]
16.03/0.18	15.61/0.17	2.7
23.06/0.26	22.38/0.25	3.0
29.46/0.33	28.62/0.32	2.9
35.44/0.39	34.39/0.38	3.0
40.94/0.46	39.68/0.44	3.2
46.02/0.51	44.59/0.50	3.2

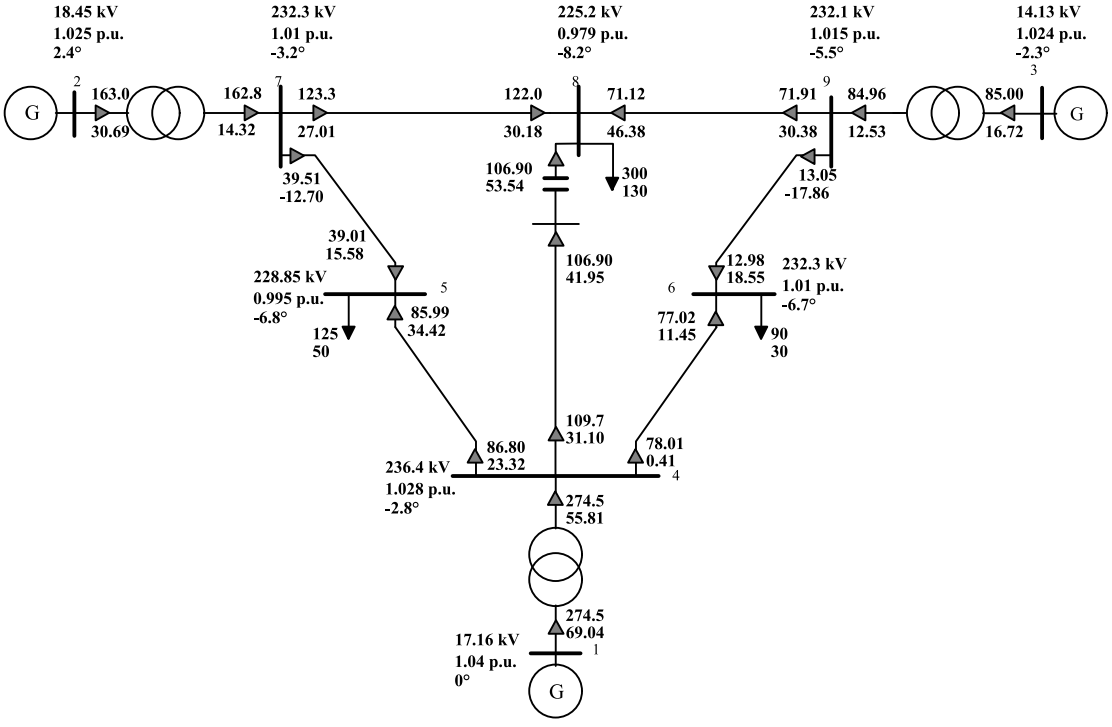

Fig. 13. 9-bus, 230 kV modified IEEE network. Load flow results with series compensation on line 4–8 ($x_c = 40.94$ Ohm, $K_s = 0.46$). Line 4–8 target flow 130 % of base case ($k = 1.3$).

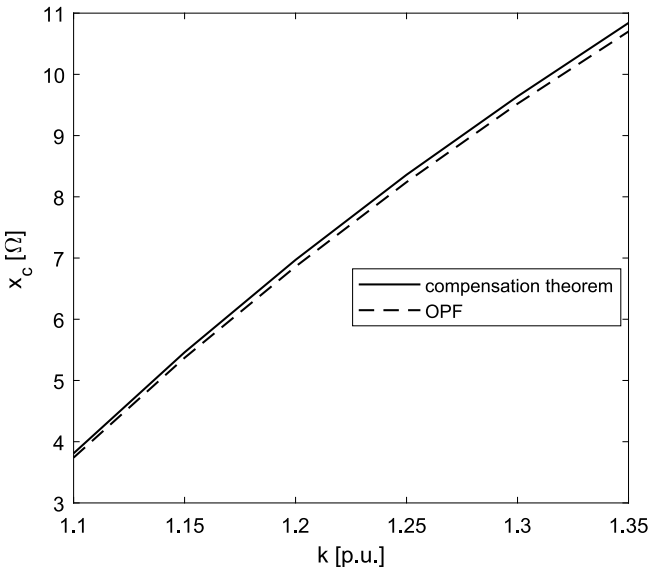

Fig. 14. 400 kV 6-node test network. Values of x_c computed with the proposed method and with the OPF, as a function of k.

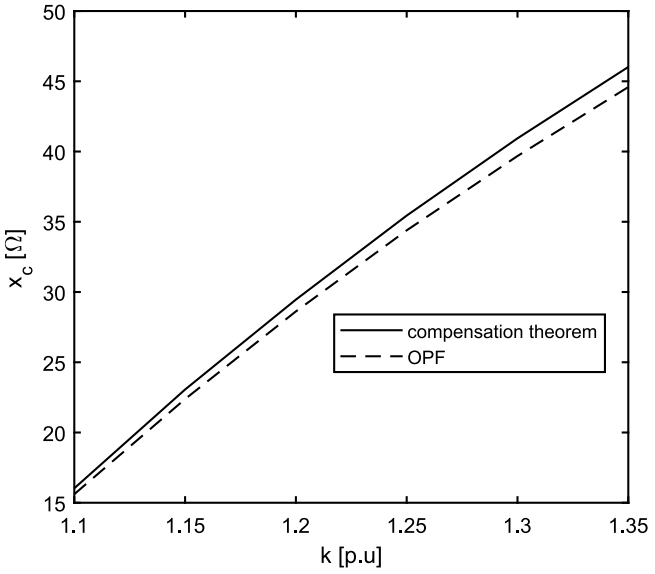

Fig. 15. 230 kV 9-node test network. Values of x_c computed with the proposed method and with the OPF, as a function of k.

increase this power by 35 % ($k = 1.35$) i.e. to obtain P^*=47.7 MW, the required capacitive reactance is $x_c = 45.39\ \Omega$ according to the proposed method, and $x_c = 44.48\ \Omega$ according to the OPF. The error is 2.05 %.

In any case (and also in many other cases not reported here), the difference (error) between the values of capacitive reactance computed with the proposed method and the standard OPF keeps always reasonably limited, and in the worst case lower than 4 %. These results demonstrate the robustness of the proposed method.

6. Conclusions

The paper deals with the series capacitive compensation as a mean to increase the power transported by transmission lines. The loadability curves of transmission lines are analyzed in the first part of the work, emphasizing the loadability increase that can be achieved by means of series compensation. The original contribution consists in the analytical derivation of the loadability curves expressed as a function of the compensation reactance, in contrast with the numerical approach usually adopted. The analytical approach proposed provides power system planners with a useful alternative tool for steady-state analysis of a transmission line.

In the second part of the paper, the line selected for series compensation is analyzed in the context of a meshed transmission system. Aiming to increase by a desired amount the power transported by the selected line, the required capacitive reactance is evaluated resorting to an original methodology based upon the compensation theorem. The method is a quick useful support and verification tool that can be added to the classic power flow methods. The validity of the method is supported by several numerical applications carried out on two test networks: the comparison of the results yielded by a standard optimization procedure and by the simpler and faster analytical procedure proposed shows the effectiveness and the accuracy of the novel method.

CRediT authorship contribution statement

Fabio Massimo Gatta: Methodology, Conceptualization, Data curation, Validation, Supervision, Writing – review & editing. **Davide Lauria:** Methodology, Conceptualization, Data curation, Validation, Supervision, Writing – review & editing. **Stefano Quaia:** Methodology, Conceptualization, Data curation, Validation, Supervision, Writing – review & editing. **Stefano Lauria:** Methodology, Conceptualization, Data curation, Validation, Supervision, Writing – review & editing.

Declaration of Competing Interest

The authors declare that they have no known competing financial interests or personal relationships that could have appeared to influence the work reported in this paper.

Data availability

Simulation data are reported in paper.

Appendix

A.1. 400 kV, 6-nodes network data

Table 7 and 8 respectively report line and load data for the 400 kV test network. Lines 1–2, 2–3 and 2–5 are double circuits on different towers; data refer to one of the circuits. The four single-circuit lines 1–4,

Table 7
400 kV test network: lines data.

Lines	V_n [kV]	Length [km]	R_1 [Ω/km]	X_1 [Ω/km]	C_1 [nF/km]	Number and code of phase subconductors	SIL at 400 kV [MVA]	Current at thermal limit [kA]
1–2, 2–3, 2–5	400	100	0.0209	0.266	13.78	3 – Cardinal	644	2.038
1–4	400	50	0.0322	0.322	11.5	2 – Cardinal	534	1.359
4–5	400	70	0.0322	0.322	11.5	2 – Cardinal	534	1.359
5–6	400	25	0.0322	0.322	11.5	2 – Cardinal	534	1.359
3–6	400	100	0.0322	0.322	11.5	2 – Cardinal	534	1.359

Table 8
400 kV test network: loads data.

Load bus	V_n [kV]	P_L [MW]	Q_L [MVAR]
2	400	1000	500
5	400	3000	1000
6	400	500	250

4–5, 5–6 and 3–6 are equipped with twin bundle conductors, whereas the three double-circuit lines are equipped with triple bundle conductors.

A.2. 230 kV, 9-nodes network data

Line, transformer, and load data for the 230 kV, 9-nodes test network are reported in Tables 9–11 respectively.

Table 9
230 kV test network: lines data (all p.u. values on a 100 MVA base).

Lines	V_n [kV]	R_1 [p.u.]	X_1 [p.u.]	$B_1/2$ [p.u.]
7–8	230	0.0805	0.072	0.0745
8–9	230	0.0119	0.1008	0.1045
7–5	230	0.032	0.161	0.153
5–4	230	0.010	0.085	0.088
4–6	230	0.017	0.092	0.079
6–9	230	0.039	0.170	0.179
4–8*	230	0.020	0.170	0.177

* Not present in the original WSCC standard 9-bus network.

Table 10
230 kV test network: transformers data.

XFMR	V_{n1} [kV]	V_{n2} [kV]	X_{sc} [p.u.]
2–7	18	230	0.0625
1–4	16.5	230	0.0576
3–9	13.8	230	0.0586

All p.u. values on a 100 MVA base.

Table 11
230 kV test network: loads data.

Load bus	V_n [kV]	P_L [MW]	Q_L [MVAR]
8	230	300*	130*
6	230	90	30
5	230	125	50

*100 MW and 35 MVAR in the original WSCC network.

References

[1] St. Clair HP. Practical concepts in capability and performance of transmission line. In: Proc. AIEE Pacific General Meeting, Vancouver, BC, Canada, 1–4 Sept 1953.
[2] Dunlop RD, Gutman R, Marchenko PP. Analytical development of loadability characteristics for EHV and UHV transmission lines. IEEE Trans PAS 1979;98:606–13.
[3] Kundur P. Power System Stability and Control. New York: McGraw-Hill; 1994.
[4] Lauria D, Mazzanti G, Quaia S. The Loadability of Overhead Transmission Lines. Part I: Analysis of Single-Circuits. IEEE Trans PWRD 2014;29:29–37.
[5] Lauria D, Mazzanti G, Quaia S. The Loadability of Overhead Transmission Lines. Part II: Analysis of Double-Circuits and Overall Comparison. IEEE Trans PWRD 2014;29:518–24.
[6] Quaia S. Critical analysis of line loadability constraints. Int Trans Electr Energy Syst 2018;28:1–11.
[7] Dong-Min K, In-Su B, Jin-O K. Determination of available transfer capability (ATC) considering real-time weather conditions. Eur Trans Electr Power 2011;21:855–64.
[8] Kay TW, Sauer PW, Smith RA. EHV and UHV line loadability dependence on VAR supply capability. IEEE Trans PAS 1982;101:3568–75.
[9] Lauria D, Quaia S. Loadability increase in radial transmission lines through reactive power injection. In: Proc. 6th International Conf. on Clean Electrical Power (ICCEP), Santa Margherita Ligure, Italy, 27–29 June 2017.
[10] El-Metwally MM, El-Emary AA, El-Azab MA. A linear programming method for series and shunt compensation of HV transmission lines. Eur Trans Electr Power 2005;15:157–70.
[11] Rajaraman R, Alvarado F, Maniaci A, Camfield R, Jalali S. Determination of location and amount of series compensation to increase power transfer capability. IEEE Trans PWRS 1998;13:294–9.
[12] Noroozian M, Andersson G. Power flow control by use of controllable series components. IEEE Trans on Power Delivery 1993;8(3):1420–9.
[13] Chansareewittaya S, Jirapong P. Power transfer capability enhancement with optimal maximum number of facts controllers using evolutionary programming. In: 37th Annual conference on IEEE industrial electronics society; 2011. p. 4733–8.
[14] Albatsh FM, Mekhilef S, Ahmad S, Mokhlis H, Hassan M. Enhancing power transfer capability through flexible AC transmission system devices: A review. Front Inf Technol Electr Eng 2015;16:658–78.
[15] Sharma A, Chanana S, Parida S. Combined optimal Location of FACTS controllers and loadability enhancement in competitive electricity markets using MILP. In: IEEE Power Engineering Society General Meeting, 2005, 2005, pp. 670-677 Vol. 1, doi: 10.1109/PES.2005.1489247.
[16] Singh JG, Singh SN, Srivastava SC. Placement of FACTS controllers for enhancing power system loadability. In: Proc. 2006 IEEE Power India Conference, New Delhi, India; 2006.
[17] Rashed GI, Shaheen HI, Cheng SJ. Optimal location and parameter setting of multiple TCSCs for increasing power system loadability based on GA and PSO techniques. In: 2007 IEEE Int. Natural Computation Conf. (ICNC'07), Aug. 24–27, 2007, vol. 4, pp. 335–344.
[18] Nagalakshmi S, Kamaraj N. Secured loadability enhancement with TCSC in transmission system using computational intelligence techniques for pool and hybrid model. Appl Soft Comput 2011;11(8):4748–56.
[19] Ghahremani E, Kamwa I. Optimal placement of multiple-type FACTS devices to maximize power system loadability using a generic graphical user interface. IEEE Trans PWRS 2013;28:764–78.
[20] Tlijani K, Guesmi T, Abdallah HH. Optimal number, location and parameter setting of multiple TCSCs for security and system loadability enhancement. In: 10th Int Multi-Conf Syst, Signals Devices (SSD), Mar 2013:1–6.
[21] Ismail B, Abdul Wahab NI, Othman ML, Radzi MAM, Naidu Vijyakumar K, Mat Naain MN. A Comprehensive Review on Optimal Location and Sizing of Reactive Power Compensation Using Hybrid-Based Approaches for Power Loss Reduction, Voltage Stability Improvement, Voltage Profile Enhancement and Loadability Enhancement. IEEE Access 2020;8:222733–65.
[22] Jebaraj L, Rajan CCA, Sakthivel S. Real power loss and voltage stability limit optimization incorporating TCSC and SVC through DE algorithm under different operating conditions of a power system. IOSR J Electr Electron Eng 2012;1:16–25.
[23] Basu M. Multi-objective optimal power flow with FACTS devices. Energy Convers Manage 2011;52(2):903–10.
[24] Samimi A, Naderi P. A new method for optimal placement of TCSC based on sensitivity analysis for congestion management. Smart Grid Renew Ener 2012;3:10–6.
[25] Siddiqui AS, Khan MT. Determination of optimal location of TCSC and STATCOM for congestion management in deregulated power system. Int J Syst Eng Manag 2016;8:1–8.
[26] Raj S, Bhattacharyya B. Optimal placement of TCSC and SVC for reactive power planning using whale optimization algorithm. Swarm Evol Comput 2018;40:131–43.
[27] Kazemi A, Badrzadeh B. Modeling and simulation of SVC and TCSC to study their limits on maximum loadability point". Int J Electrical Power & Energy Systems 2004;26(5):381–8.
[28] Lauria D, Mottola F, Quaia S. Analytical Description of Overhead Transmission Lines Loadability. Energies 2019;12:3119.
[29] Norma CEI 11-60. *Portata al Limite Termico Delle Linee Elettriche Aeree Esterne con Tensione Maggiore di 100 kV*, 2nd ed., Comitato Elettrotecnico Italiano: Milano, Italy; 2002 (In Italian).